N92-14079

COBE GROUND SEGMENT ATTITUDE DETERMINATION

V. K. Kumar, I. Freedman (ST Systems Corporation, Lanham, MD 20706)
E. L. Wright (UCLA, Los Angeles, CA 90024)
F. S. Patt (GSC, Laurel, MD 20707)

ABSTRACT

The COsmic Background Explorer (COBE) spacecraft was launched in November 1989 by NASA to survey the sky for primordial radiation left from the "Big Bang" explosion. The success of the mission requires an accurate determination of the spacecraft attitude. While the accuracy of the attitude obtained from the attitude sensors is adequate for two of the experiments, the higher-accuracy attitude required by the Diffuse InfraRed Background Experiment (DIRBE) is obtained by using the DIRBE instrument as a special type of star sensor. This paper presents an overview of the attitude processing algorithms used at the Cosmology Data Analysis Center (CDAC) and discusses some of the results obtained from the flight data.

1.0 INTRODUCTION

The COsmic Background Explorer (COBE) spacecraft was launched by NASA in November 1989 to survey the sky for primordial radiation left from the Big Bang. The spacecraft carried three very sensitive instruments: (1) the Diffuse InfraRed Background Experiment (DIRBE) to survey the sky in the 1 to 300 micrometers wavelength in ten bands; (2) the Far InfraRed Absolute Spectrophotometer (FIRAS) to survey the sky in the 0.1 to 10 millimeter wavelength bands; and (3) the Differential Microwave Radiometer (DMR) to determine whether the primordial explosion was equally bright in all directions. The FIRAS and DIRBE are enclosed in a liquid helium cryostat to provide a stable low-temperature environment. These three instruments, along with the cryostat and the shield to protect the instruments from illumination by the Sun and Earth, form the upper half of the spacecraft (instrument module) (Figure 1). The lower half of the spacecraft (spacecraft module) includes the mechanical support structure, the attitude control system, the instrument and spacecraft electronics, and the solar cell arrays.

The COBE was placed into a circular Sun-synchronous orbit 900 km above the surface of the Earth. The spacecraft crosses the equator from north to south at approximately 6 a.m. local time. The orbit of the spacecraft is inclined 99 degrees to the equator and precesses to follow the apparent motion of the Sun relative to the Earth.

The COBE spacecraft rotates about the spacecraft X-axis at approximately 0.815 rpm. The COBE attitude control system points the spin axis (FIRAS line of sight) at approximately 94 degrees away from the Sun and in a generally outward direction from the Earth. The spacecraft rotation allows DIRBE and DMR to observe half the sky every orbit, as their lines of sight are 30 degrees away from the spin axis.

The COBE attitude control system is composed of: (1) attitude sensors: two-axis Digital Sun Sensors (DSS), infrared Earth-horizon Scanner Assemblies (ESA), rate integrating gyros, and Three-Axis Magnetometers (TAM); (2) attitude controllers: reaction wheels, electromagnets (torquer bars), and a pair of large rotating momentum wheels; and (3) a set of control electronics. Figure 2 shows the COBE attitude sensor and control system geometric configuration. The three control axes lie in a plane perpendicular to the spacecraft spin axis and are labeled A, B, and C. The reaction wheels control the spacecraft spin axis orientation by applying controlled torques along these axes. The large momentum wheels are used to control the spacecraft spin rate and to maintain approximately zero net angular momentum about the X-axis. The electromagnets provide control torques from the Earth's magnetic field to discharge the angular momentum build-up in the reaction and momentum wheels. The electronics and data handling systems on the spacecraft collect the data from the instruments and attitude sensors and transmits these data to the ground. The complete data stream is recorded on two on-board tape recorders and played back to the ground-receiving station at Wallops Flight Facility once (or twice) per day. In addition, the spacecraft is monitored periodically in realtime and commands are sent to it through the Tracking and Data Relay Satellite System (TDRSS).
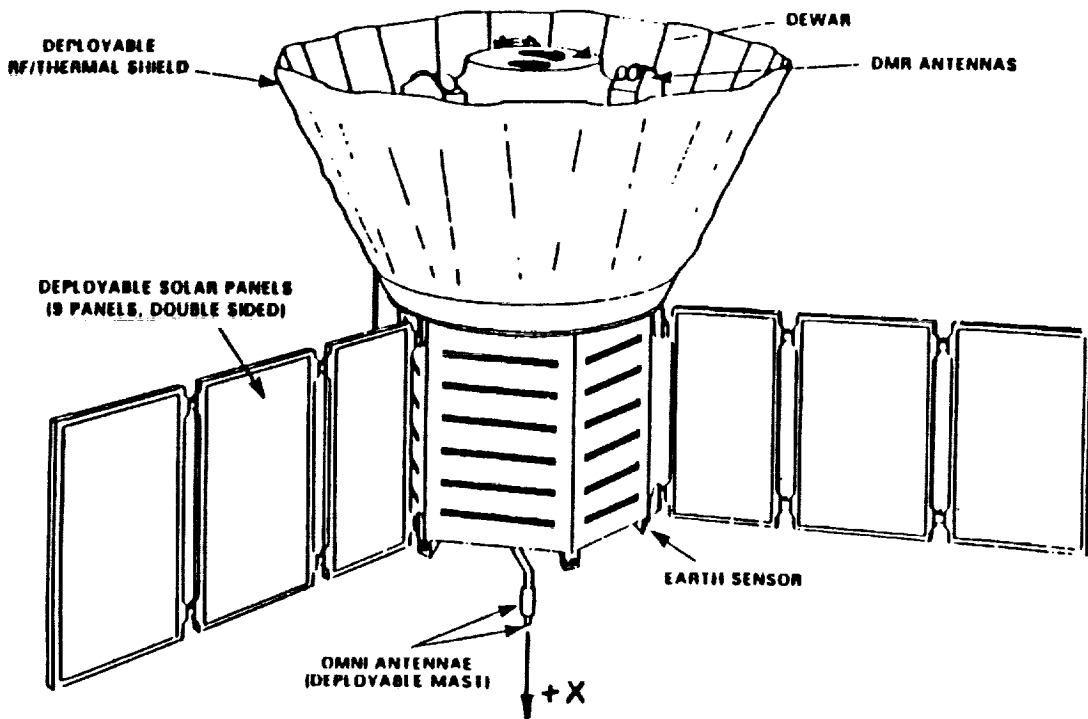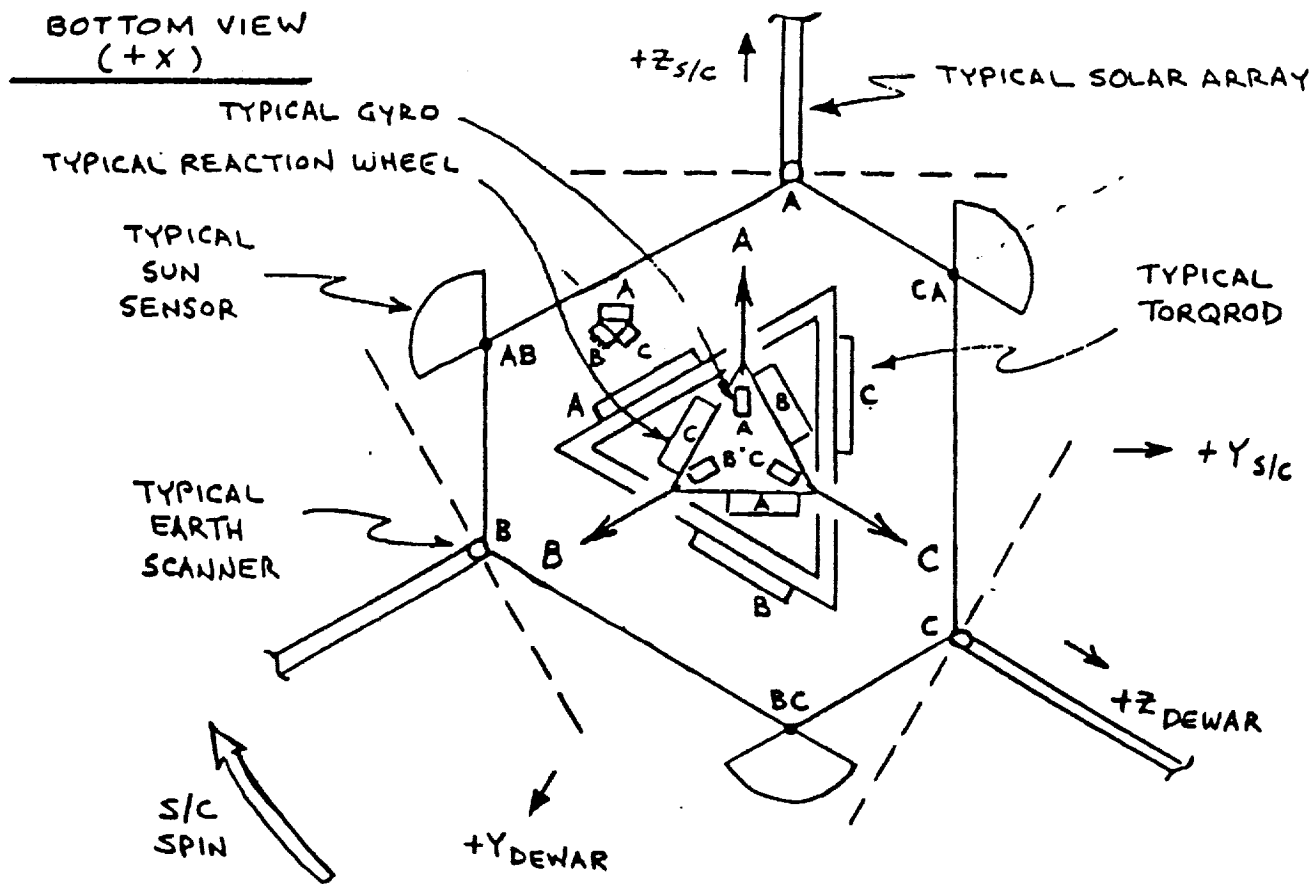
Figure 1. COBE Observatory Deployed

Figure 2. COBE Attitude Control System (ACS) Configuration

The ground reconstruction of the spacecraft attitude for instrument data interpretation is performed at the NASA Cosmology Data Analysis Center (CDAC). This paper presents an overview of the CDAC attitude processing algorithms and discusses some of the results obtained from flight data.

2.0 PROCESSING ALGORITHMS

The initial estimate of the spacecraft attitude is obtained by processing the attitude sensor data. The initial attitude estimate is also called the "coarse aspect". The accuracy of the coarse aspect is further improved using the DIRBE instrument payload data in the telemetry. This refined attitude is called the "DIRBE fine aspect".

2.1 Coarse Aspect

The coarse aspect is derived from the Sun sensor, Earth scanner, and gyro measurements. Observation vectors required in the attitude computation are constructed from the sensor measurements. The inertial reference vectors are constructed using analytical methods. The Q-method (QUEST) (References 1, 9) is used to obtain an epoch attitude from observation vectors and reference vectors. The attitude at other times is obtained by propagating the epoch attitude to the observation times using the body angular velocity derived from the gyro measurements.

2.1.1 Observation Vectors Computation

There are six two-axis digital Sun sensors (DSS) on the COBE spacecraft. Three of the DSS's serve as primary sensors, and the other three serve as backups. The alignment of the sensor axes with respect to the spacecraft reference frame is shown in Figure 3.

Each DSS has a 128x128 degree square field-of-view (FOV). They measure the projection angles of the Sun vector in the DSS sensor reference frame. A detailed description and operation of the DSS used on COBE, as well as the procedure for obtaining the Sun vector in the spacecraft coordinate frame, are also described in Reference 1.

The spacecraft-to-Sun vector in the inertial frame is obtained by the analytical procedure described in Reference 2. The distance between the spacecraft and the Earth is neglected in computing this vector.

The COBE spacecraft has three infrared Earth-horizon Scanner Assemblies (ESA) for tracking the spacecraft nadir. A brief description and operation of the sensor can be found in Reference 3. The ESA sensor reference axes orientation in the spacecraft reference frame is as shown in Figure 4. The ESA's measure the angle between the spacecraft +X axis and the nadir vector in the sensor scan plane (split-to-index angle), which is normal to the sensor Z axis.

The ESA split-to-index angle measurement, along with the Sun observation vector computed earlier, is used to compute the spacecraft nadir angle, η (Figure 5). By using techniques of spherical trigonometry one can derive the following relation for η:

$$\cos(\eta) = \frac{cB \times cP + sB \times cF \times \sqrt{(sB^2 \times cF^2) + cB^2 - cP^2}}{(sB^2 \times cF^2) + cB^2} \qquad (1)$$

$s(\ ) = \sin(\ );\ c(\ ) = \cos(\ );\ B, P, F$ are the angles defined in Figure 5.

The nadir vector direction in the ESA sensor reference frame is then given by

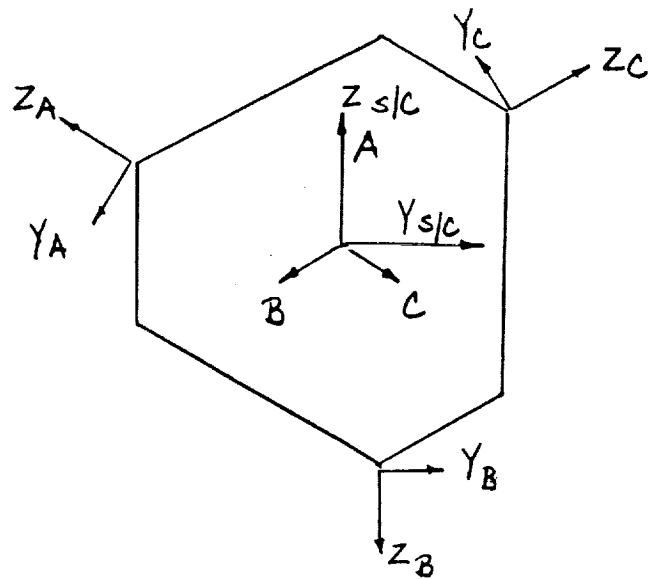$$\hat{N}_{ESA} = [s\eta \times cA,\ s\eta \times sA,\ c\eta]^T. \qquad (2)$$
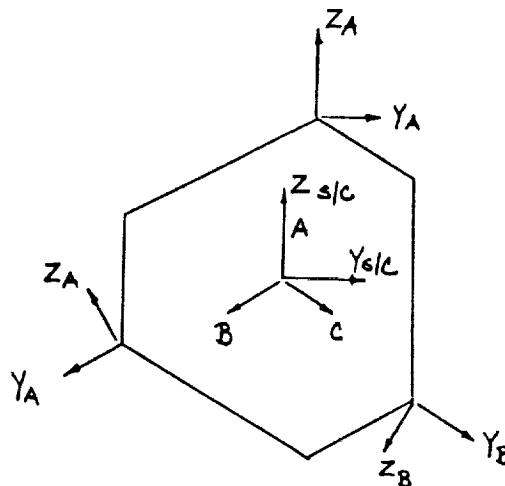
Figure 3. DSS Axes Orientation

Figure 4. ESA Axes Orientation

$X_s Y_s Z_s$ - Sensor axes
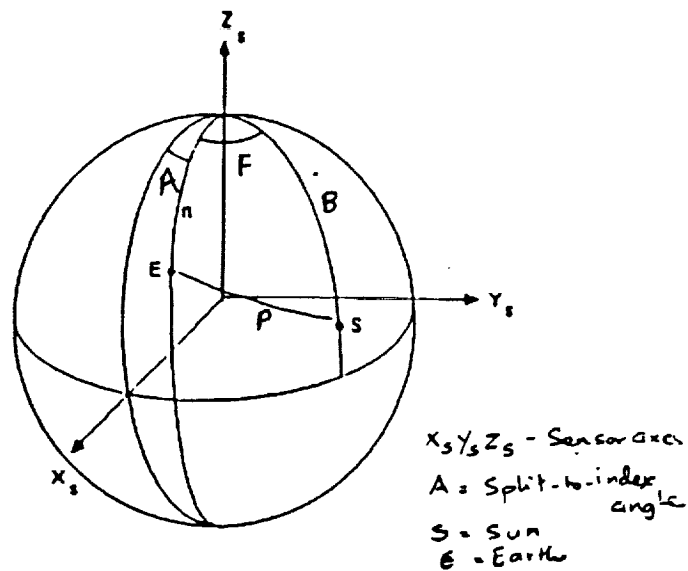A = Split-to-index angle
S = Sun
E = Earth

Figure 5. Geometry for Nadir Vector Computation

The nadir vector in the spacecraft reference frame is obtained by premultiplying N by the sensor-to-spacecraft alignment matrix. It can be noted that two solution vectors exist for each split-to-index angle measurement (one for each value of η). The correct nadir solution vectors cluster very closely in the spacecraft reference frame. The effective nadir vector is taken as the average of all the correct solution vectors.

The spacecraft nadir vector in the inertial frame is obtained from the spacecraft orbit data computed by the Goddard Space Flight Center's Flight Dynamics Facility (FDF) (Reference 4).

2.1.2 Spacecraft Body Angular Velocity

The COBE spacecraft has six single-axis rate integrating gyros for spacecraft body angular velocity measurements. The gyro input axes are oriented in the spacecraft frame as shown in Figure 6. For ground processing, measurements from only one of the three X-axis gyros is telemetered to the ground. The X-axis gyro selected for the telemetry is commanded from the ground. Currently, of the three control axis gyros, only A- and C-axis gyros are active. The B-axis gyro failed in flight a few days after the launch.

The spacecraft angular velocity component in the direction of the gyro input axis is related to the gyro measurement of this quantity, W_i, by

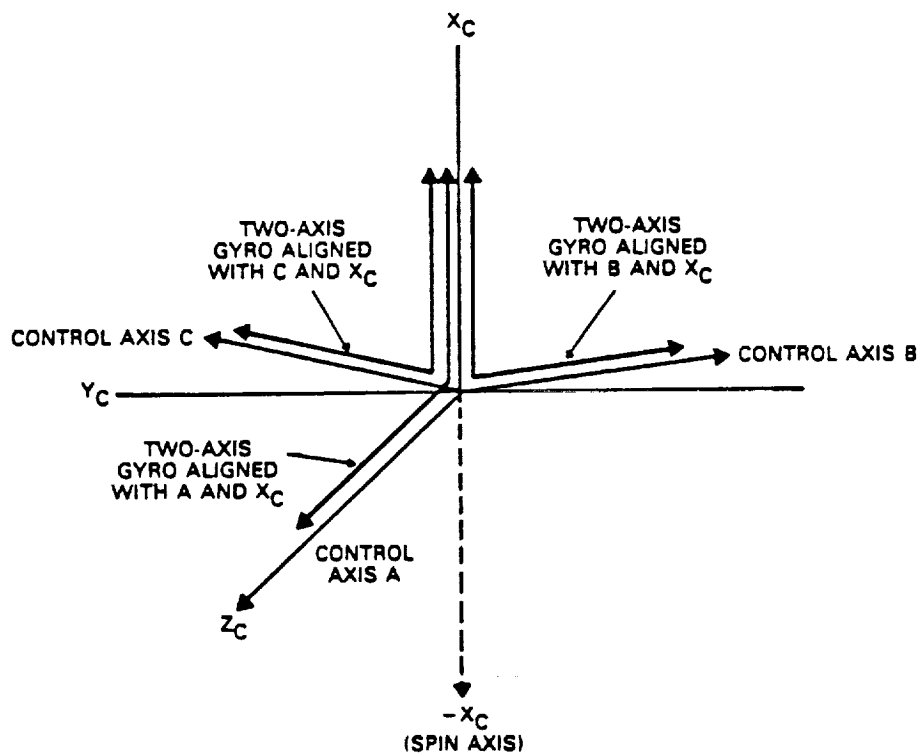$$W_i = (1 + K_i)\hat{U}_i\bar{W}_i + N_i + B_i \qquad (i = A, C, X) \qquad (3)$$

Figure 6. Gyro Input Axes Orientation

155

where U's are unit vectors in the direction of the gyro input axes in the spacecraft body frame; W is the true body angular velocity vector; B designates the gyro rate biases; K represents the gyro scale factors; and N specifies the gyro output noise terms, which are assumed to be negligible. The direction vectors of the gyro input axes are obtained from the pre-launch alignment measurements of the gyro input axes. Given the values of gyro drift rate biases and the scale factors, the above set of linear equations can be solved for the components of the spacecraft angular velocity in the spacecraft body frame. Estimation of COBE gyro drift rate biases and scale factors are discussed in Reference 5.

2.1.3 Attitude Computation

The coarse aspect determination procedure is based on the key assumption that the error in the modeling of the spacecraft motion using gyro data is smaller than the error in the sensor data. The procedure uses all the Sun and nadir vectors in a batch process to determine the spacecraft attitude at an epoch time and uses spacecraft body angular velocities to propagate the epoch attitude to other times. This method has been used successfully in other spacecraft missions (see Reference 7).

Assume that we have a set of vector observations resolved in the body frame: W1, W2,...Wn at times T1, T2,... etc., as well as the corresponding reference vectors in the inertial frame (e.g., GCI). Assume also that we have gyro data synchronized to the observation times, and that the calibrations of the gyros (scale factors, alignments, and drift rates) are reasonably well known. We wish to compute an attitude at some epoch time (assume T1 for convenience, but it could be any time in the interval).

Take some initial attitude estimate at time T1; this could be the result of a single-frame attitude algorithm or could be completely arbitrary, since the QUEST algorithm is linear and, therefore, does not depend on the initial estimate. Express the estimate as a quaternion Q1 (see Reference 1 for quaternion definition). Use the gyro data to compute rotation quaternions between the observation times: Q12, Q23, etc. Propogate the initial estimate to the observation times

$$Q2 = Q1 \times Q12,$$
$$Q3 = Q1 \times Q12 \times Q23, etc. \tag{4}$$

The propagated quaternions are used to rotate the observation vectors to the inertial frame at T1. This can be done by calculating the rotation matrix [A] corresponding to each Q and multiplying the observation vectors by the inverse of the matrix; i.e.,

$$Wk' = inv[A(Qk)] Wk, \quad (k = 1, 2, ...). \tag{5}$$

All of the transformed observation vectors and the reference vectors are used as input to the QUEST algorithm and a correction quaternion DQ is computed. The initial estimate is then corrected by quaternion multiplication

$$Q1' = DQ \times Q1. \tag{6}$$

Any of the other propagated quaternions can be corrected in the same sense to provide attitude estimates at other observation times.

2.2 DIRBE Fine Aspect

The DIRBE fine aspect determination system uses the DIRBE experiment as a star tracker to improve the accuracy of the coarse aspect solutions. The DIRBE field-of-view (FOV) traces a helical scan path in the sky. The fine aspect determination procedure consists of identifying stars that pass through the DIRBE FOV and then correcting the coarse attitude using these identified stars as attitude reference points.

2.2.1 DIRBE Star Identification

The DIRBE data in the short wavelength (1.25-5.0 micron) bands contain a large number of peaks due to star passages across the instruments' FOV, as well as sharp spikes due to cosmic rays and broader peaks due to the galactic plane and extended sources. Of the three short wavelength DIRBE bands, one has the greatest a priori knowledge of the sky in the K-band (2.2 micron) because of the Two Micron Sky Survey (TMSS) (Reference 8). Hence, the DIRBE data from the K-band channels was chosen for star identification.

In order to separate DIRBE star peaks from the broader peaks due to galactic plane and extended sources, DIRBE data is passed through a non-recursive filter ("matched filter") of the form

$$Y_k = \sum_i^L W_{k-i} \times \frac{X_{k-i}}{G_k}, \quad (k=1,2,...),$$

(7)

where Y is the filter output; X represents the DIRBE measurements; W represents the filter weights; G_k is the filter output normalizing gain and L is the filter length.

The filter length, L, is determined by the width of the DIRBE star passage given by (DIRBE FOV size)*(DIRBE sampling rate)/(DIRBE scan speed). The DIRBE instrument has a 0.7 x 0.7 degree square FOV. The DIRBE samples are telemetered at the rate of eight samples per second. Since the DIRBE optical axis is inclined at 30 degrees to the spacecraft X-axis, the DIRBE scan speed on the sky is half the spacecraft spin rate. At the spacecraft nominal spin rate of 0.815 rpm, the DIRBE star peak is 2-3 samples wide. In the present work, the filter length is chosen to be eight samples with the following set of filter weights: W=(-1,-1,3/4,5/4,5/4,3/4,-1,-1). Note that the filter output is zero for constant input signals as well as input ramps. Also, with the filter length of 8 samples, the confusing sources more than 2 degrees away will be outside the filter window.

The filter output normalizing gain function, G_k is chosen as

$$G_k = Min[32767, 1.1G_{k-1} + 1] \qquad \text{if } 100|Y_k| > G_{k-1}$$

$$= Max\left[1.5, \frac{G_{k-1}}{1.1}\right] \qquad \text{otherwise.}$$

(8)

The value of G(0) is arbitrary. In between star peaks, the matched filter output tracks the background noise in the DIRBE data. The gain algorithm then dampens the response to the filter output, thereby normalizing the star peak intensity to the current estimated noise level.

The filtered DIRBE signal from all the selected channels is scanned for candidate star peaks using the following selection criteria:

1) The peak flux should be greater than a specified minimum.

2) The signal should peak in all the selected DIRBE channels simultaneously. This ensures rejection of spikes due to charged particles.

The time of the star observation at a candidate star peak is computed as

$$T_p = T(k) - \frac{[(L-1)/2 - N(k)]}{8}$$

(9)

where N(k) is the star position (in number of DIRBE samples) within the last L data points (centroid). The centroid in each of the DIRBE channels is computed as

$$C_k = \sum_{j=1}^{L} f_{k-1} * X_{k-1} / \sum_{j=1}^{L} g_{k-1} * X_{k-1}.$$

(10)

for L=8, f=(5/12,5/12,-3/2,-1/2,1/2,3/2,-5/12,-5/12) and g=(-1,-1,1,1,1,1,-1,-1). The effective centroid is taken as the average centroid of all the selected DIRBE channels.

The approximate DIRBE line-of-sight (LOS) direction (in the inertial frame) at the star observation time, T_p, is defined by the unit vector

$$\hat{U}_p = A_{IB} \times A_{BD} \times \hat{U}_D$$

(11)

where: $\hat{U}_D$ is the DIRBE LOS in the DIRBE reference frame.

A_{BD} = rotation matrix to go from the DIRBE frame to the spacecraft body frame (derived from the DIRBE alignment data).

A_{IB} = rotation matrix to go from spacecraft body frame to inertial frame (derived from the coarse attitude).

The DIRBE fine aspect star catalog is searched for a star that lies very close (within a predefined search radius) to U_p. The fine aspect star catalog contains 1207 bright stars selected from TMSS, Smithsonian Astrophysical Observatory (SAO), and IRAS point source catalogs. The selection was based on the following three criteria (Reference 6):

1) the K-magnitude < 3.0. This ensures that a measured 2.2 micron flux exist for most sources.

2) RMS centroiding error less than 1.5 arc-min, as determined from the effects of other stars near the bright star.

3) No brighter neighbors within a 1.75 degree radius. Because the nearest star to the coarse attitude position is assumed to be the identified star, stars with brighter neighbors should be avoided.

If the catalog search fails to find a star to associate with a candidate star peak, then that peak is dropped and is labeled as "false peak".

2.2.2 DIRBE Differential Correction

The differential correction consists of finding small corrections to the coarse attitude using the DIRBE identified known stars as attitude references. The attitude error can be represented as an inertial vector (Reference 7). If we assume that the error due to the imperfect modeling of the spacecraft motion by the gyros is negligible, then the coarse attitude error can be represented by constant rotation in the inertial frame. The following differential correction procedure is based on this key assumption.

Let dA denote the constant rotation matrix which takes the coarse attitude predicted body frame to the true body frame. Assuming that this rotation is small, one can write

158

$$dA = \begin{bmatrix} 1 & c & -b \\ -c & 1 & a \\ b & -a & 1 \end{bmatrix} \qquad (12)$$

where a, b, and c are small angle rotations about the body x, y, and z axes, respectively. Thus, the differential correction problem is reduced to finding the three small rotation angles a, b, and c.

If we define a vector, $\bar{P}$ = transpose [a, b, c], then the change in any unit vector, $\hat{V}$, under the action of dA is given by

$$d\hat{V} = \bar{P} \times \hat{V} \qquad . \qquad (13)$$

Assume that N DIRBE star sightings have been identified after processing the DIRBE raw data. Then

$$\hat{O}_k - \hat{D}_k = \bar{P} \times \hat{D}_k, \qquad (k=1,...,N), \qquad (14)$$

where $\hat{O}$ is the unit vector to the kth DIRBE sighted star, and $\hat{D}$ is the unit vector along the DIRBE LOS predicted by the coarse attitude at the kth star observation time.

It is also true that

$$\langle \hat{O}_k - \hat{D}_k, \; \bar{W}_k \times \hat{D}_k \rangle = \langle \bar{P} \times \hat{D}_k, \; \bar{W}_k \times \hat{D}_k \rangle, \qquad (15)$$

where $\bar{W}$ is the body angular velocity at the kth star observation time and $\langle,\rangle$ denotes the scalar product of two vectors. The left-hand side of the above equation is the along scan component of the vector representing the deviation of the coarse attitude-predicted DIRBE LOS vector from the vector pointing to the DIRBE sighted star.

Using techniques of vector algebra, the right-hand side of Equation (15) can be written as

$$\langle \bar{P} \times \hat{D}_k, \; \bar{W}_k \times \hat{D}_k \rangle = \langle \bar{P}, \; \bar{E}_k \rangle \qquad (16)$$

where $\bar{E}_k = \bar{W}_k - \hat{D}_k \langle \hat{D}_k, \bar{W}_k \rangle$ denotes a vector perpendicular to $\hat{D}_k$ in the plane formed by $\bar{W}_k$ and $\hat{D}_k$.

One can set up the following N-linear equations, one corresponding to each DIRBE-sighted star, for the three unknowns a, b, and c:

$$\langle \bar{P}, \; \bar{E}_k \rangle = \langle \hat{O}_k - \hat{D}_k, \; \bar{W}_k \times \hat{D}_k \rangle, \qquad (k=1,...,N). \qquad (17)$$

For N > 3, this will be an over-determined system which can be easily solved for a, b, and c in a least-squares sense.

The quaternion representing the differential correction rotation is given by (first order approximation)

$$dQ = \left[\frac{a}{2}, \; \frac{b}{2}, \; \frac{c}{2}, \; 1 \right] \qquad (18)$$

3.0 ANALYSIS AND PROCESSING PIPELINE PERFORMANCE USING FLIGHT DATA

A number of significant improvements to the COBE Attitude processing pipeline have resulted directly from analysis of the flight data. The most important of these are:

1)   Earth scanner acquisition-of-signal (AOS) timing adjustments

2)   Gyro calibration and temperature correction

3)   DIRBE boresight alignment

Each of these is discussed below, followed by a summary of the overall system performance.

3.1 Earth Scanner AOS Timing Adjustment

During the first several months of the mission, the coarse aspect solutions contained significant periodic pitch errors. The errors could readily be seen by projecting the fine aspect differential corrections onto the roll, pitch, and spin axes. These errors had an orbital frequency and the magnitude varied according to the time of year. The errors were not symmetric about the orbit but appeared to depend on the angle between the spin axis and the orbit plane. The maximum error was approximately 0.4 degrees at the winter solstice; the errors were small in early March 1990, but then increased to approximately 0.6 degree at the summer solstice.

It was proposed by one of us (E. Wright) that this was consistent with an average timing error of 0.25 degree (one telemetry minor frame) in the Earth-horizon scanner data, at the COBE spin rate. This prompted a detailed analysis of the Earth-horizon Scanner Assembly (ESA) data timing and, in particular, the ESA Acquisition-of-Signal (AOS) data in the ESA telemetry.

The AOS is meant to indicate the delay between the computation of each ESA Split-to-Index (SI) value and the time at which the ESA is read by the spacecraft telemetry unit. The ESA rotates at approximately 4 hz, the same as the minor frame (mF) period, so the SI data can be up to 1 mF old by the time it is sampled. In principle, the SI time tag can be corrected by the AOS to get the true sample time.

The flight data showed that the telemetered AOS seemed to contain no useful information about the SI sample times. The AOS values for all three ESA's cycled continously through the total range of 0.0 to 0.25 seconds with a period of about 11 seconds, producing a "saw-tooth" pattern. The SI values showed no behavior which correlated with the AOS cycles; in fact, correcting the SI data using the AOS resulted in obvious discontinuities in the SI data first derivatives at the AOS roll-over points. Thus the AOS data were determined to be not useful and were ignored for data processing.

Additional analysis was performed to determine if the true AOS could be derived from the data. Simulated ESA SI data were generated using ine Aspect solutions and compared with the telemetered values. Figure 7 is a plot of the differences between the telemetered and simulated values for one ESA over a 20-minute period. The oscillation in the data is produced by the spacecraft rotation period of approximately 73 seconds. The pattern in the plot is consistent with a true AOS which "rolls over" from 0.25 to zero seconds about every 10 minutes. The differences resulting from the AOS are out-of-phase with the SI data and are proportional in amplitude to the magnitude of the AOS and the amplitude of the SI data.

The difficulty with this conclusion is that there is no direct method to determine the AOS from telemetry alone. The simplest scheme from an operational standpoint was to simply average the AOS by including a constant correction of 1/2 mF (0.125 second) to the time tags. This average correction produces reasonable results if the attitude propagation intervals are longer than the AOS rollover period. Fortunately this period was shorter (about 10 minutes) than the typical solution interval (20 to 45 minutes). This average correction has produced very satisfactory results.

Figure 8 (a) shows the pitch corrections applied to the coarse aspect by the fine aspect solutions for the prelaunch definition of the AOS, while Figure 8(b) shows the corrections for the same time period using the 1/2 mF average AOS value. The pitch errors are now typically less than 0.1 degree. This has had the added benefit of allowing the star identification tolerance for the fine aspect system to be reduced, resulting in fewer misidentifications.
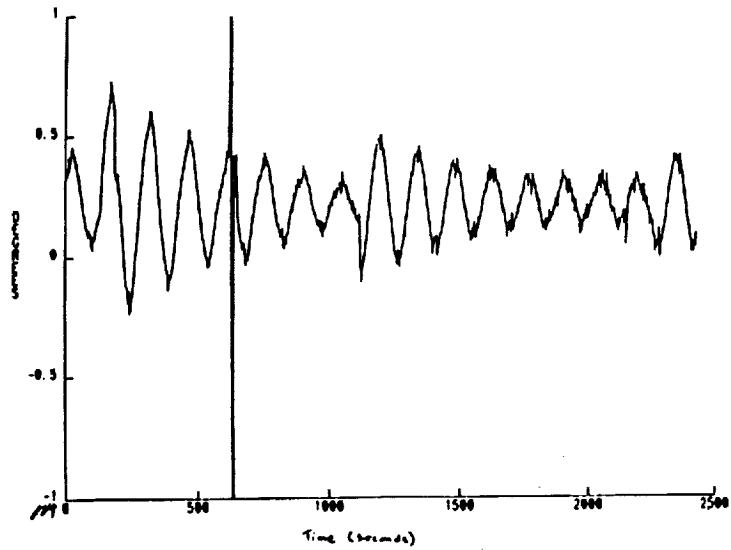
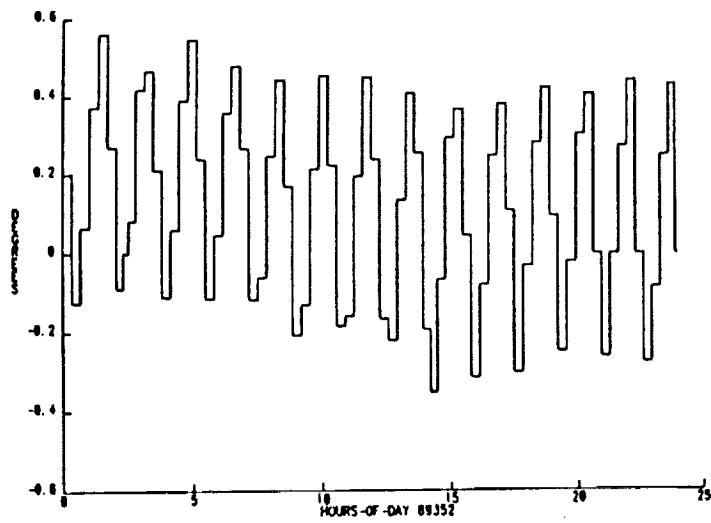**Figure 7. Difference Between Raw and Simulated ESA-A SI Data**

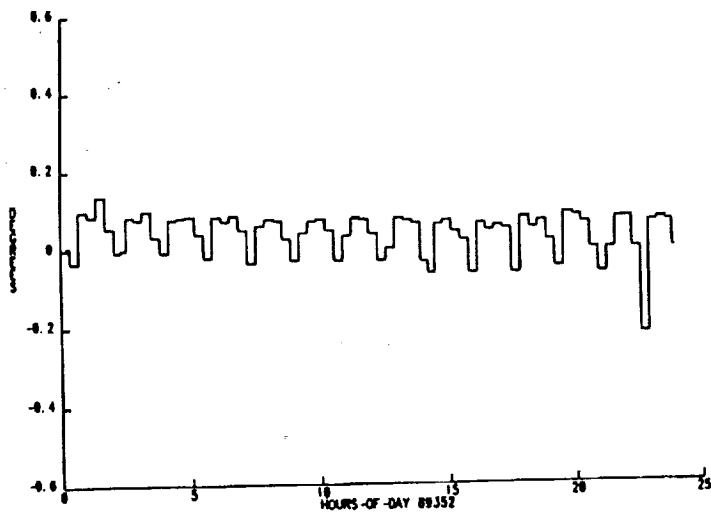**Figure 8(a). Coarse Aspect Pitch Errors (AOS From Telemetry)**

Figure 8(b). Coarse Aspect Pitch Errors (AOS=-0.125)

161

3.2 Gyro Calibration and Temperature Correction

This topic is discussed in considerable detail in Reference 5. Only the analysis and performance results will be summarized here.

For much of the first year of the mission the ground segment calibration facility was still in the development and testing stages. The attitude processing for quick-look analysis relied mainly on manual estimation of the spin axis scale factor to minimize the attitude propagation errors. While this was adequate to support the coarse requirement (1 degree 3 sigma), it was time-consuming, did not allow quick response to calibration changes, and did not support calibration of the control axis gyros. The problem was aggravated by the apparent drift in the spin axis gyro calibration, especially at the start and end of the eclipse season. At various times calibration parameters were obtained from the COBE FDF, but this was only an interim solution. The fine aspect processing from this period clearly showed the effects of the gyro propagation errors, and only in rare instances was the 3 arc-minute requirement met.

It was not until late summer 1990 that serious attention could be devoted to the attitude propagation problem. At this time the gyro calibration facility testing schedule was accelerated. At the same time, analysis was undertaken of other possible sources of propagation error, since these errors showed periodic behavior which did not seem to reflect calibration errors. This analysis culminated in the demonstration of the AX gyro scale factor/baseplate temperature correlation in August 1990, an effect that explained not only the short-term variations but also the seasonal drift. A correction for the temperature effect was included in the Attitude pipeline shortly thereafter.

With the temperature correction in place, the testing of the calibration facility was rapidly completed. The algorithm was shown to converge rapidly for two test cases: the early-mission spin-up of the spacecraft from 0.23 to 0.82 rpm, and the normal mission phase with nearly constant spin rate. The early mission results provided useful visibility on the important gyro calibration parameters (X gyro scale factor and bias and control axis gyro scale factors). This parameter set was used to initiate the normal mission calibration activities.

The results of the gyro calibration and temperature correction can be clearly seen in the observation residuals for the fine aspect solutions. As previously stated, the fine aspect solution residuals did not consistently meet the 3 arc-minute specification prior to the resolution of the gyro propagation errors. With current capabilities, the residuals Figure 9 are typically 1.5 arc-minutes (includes some error from the star centroids in the star catalog, where the criterion was 1.5 arc-minutes), half of the specification. (Note that this is after the boresight alignment adjustment, discussed in the following section.) The fine aspect residuals are also much more consistent, without the large variations in solution quality that were previously evident. Finally, the improvements in gyro propagation have also allowed the solution arcs to be increased from 20 to 45 minutes. This has allowed more DIRBE star observations to be included in each solution, improving the outlier rejection capability, and has allowed solutions to span intervals of no observation that result from DIRBE calibration activities and South Atlantic Anomaly crossings.

3.3 DIRBE Boresight Alignment

The errors of the DIRBE boresight alignment components (azimuth and elevation) were evaluated at different stages of the Attitude Pipeline analysis. The elevation (i.e., cross-scan) error became apparent soon after regular fine aspect processing was initiated. Plots of star observations in the DIRBE FOV showed that the cross-scan pattern was of approximately the width of the beam (0.7 degrees), but the average was offset from zero by about 4 arc-minutes. This offset was consistently observed in all of the fine aspect processing, so a correction of the elevation angle was approved early on for both the attitude and the DIRBE processing. This change had no effect on the fine aspect observation measurements (as only along-scan residuals are used in the fine aspect correction), and hence did not affect the solution results.
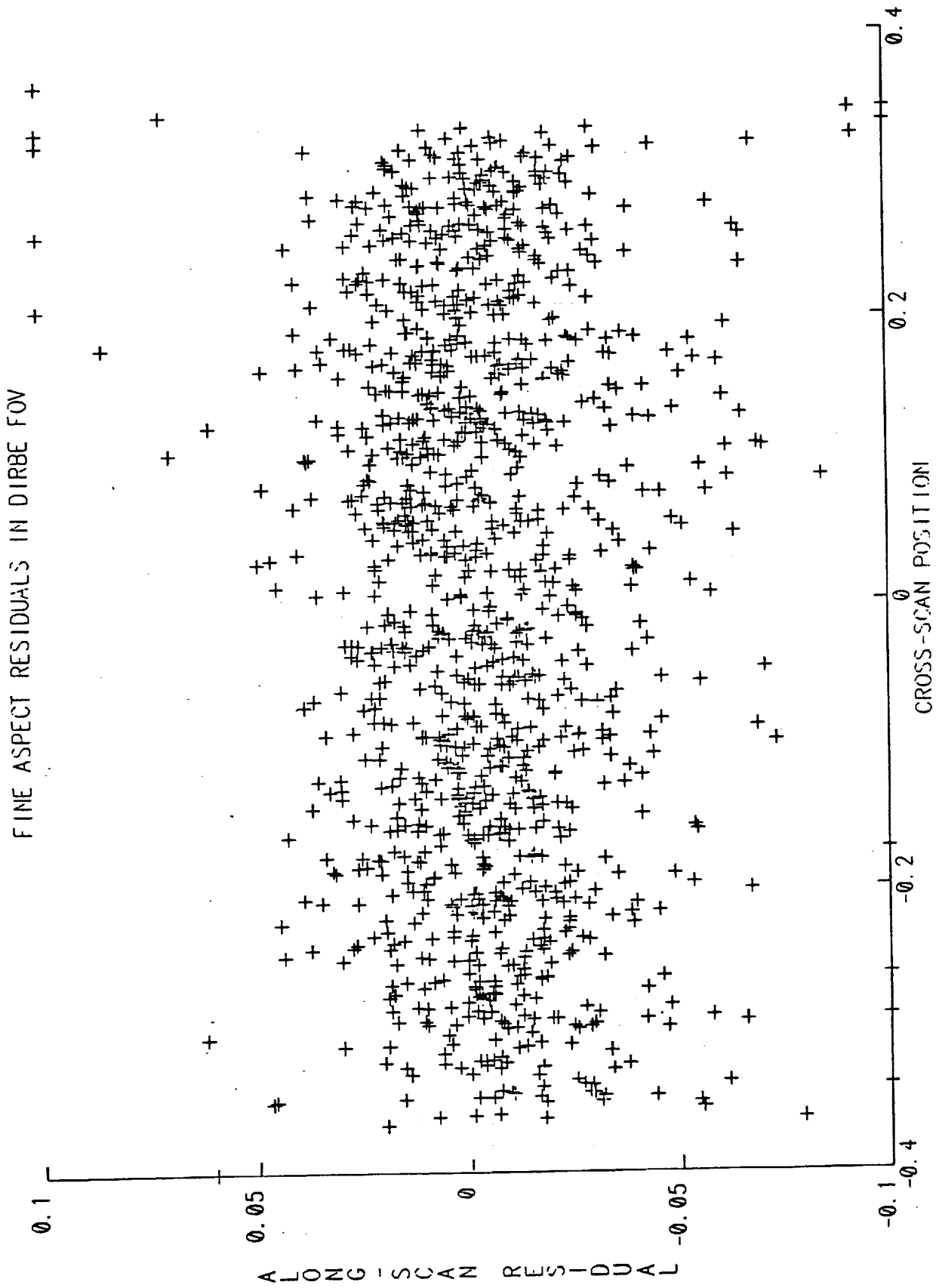
Figure 9. Fine Aspect Residuals in DIRBE FOV

163

The azimuth (along-scan) error is much more difficult to observe, since the fine aspect differential corrector is performing a least-squares minimization of the along-scan deviations. For short solution intervals, in which the total spin axis precession is not significantly greater than the size of the DIRBE scan cone, the minimization process tends to absorb most of the azimuth alignment as a component of the computed aspect correction. Since the gyro propagations remained short (20 minutes or less) and the observation residual noise was relatively large, the azimuth alignment error was not observable.

As discussed above, following the incorporation of the gyro calibration and the temperature correction, the propagation intervals were increased and the fine aspect observation noise was reduced. Under these circumstances, a consistent mean residual was observed of a magnitude of approximately 1 arc-minute. For longer propagation intervals, the rotation required to remove the mean residual introduced by an azimuth alignment error changes too much to be computed as a single rotation; in fact, for the 45-minute propagation intervals (almost half of the orbit period), the required rotation is almost completely reversed from the start to the end of the interval. Thus a significant mean residual remains even after the minimization process.

Initial experiments to nullify the mean residual used adjustments of the DIRBE data sample timing rather than the boresight azimuth; for a contant spin rate, the effects of these two changes are indistinguishable, and the design of the Attitude Pipeline made it easier to use the timing adjustment for testing purposes. It was readily found that a sample timing delay of 15 milliseconds was sufficient to reduce the mean residual to negligible values for several test intervals. This change also reduced the RMS observation residuals by about 25 percent, indicating that the retiming of the data also improved the overall fit to the error model. Note that this timing change represents along-scan boresight motion of approximately 0.036 degrees, more than twice the observed mean residual, indicating that a large part of the mean residual was still being absorbed by the least-squares fit even with 45-minute propagation intervals.

For implementation of this correction it was decided, in consultation with the DIRBE science team and the software developers, to use a correction to the azimuth alignment rather than the sample timing, as this form of the change was more easily accomodated by the system as a whole. The correction was computed to be 0.0738 degrees, equivalent to 15 milliseconds of spacecraft rotation at the average spin rate of 4.92 degrees per second. This correction was shown, as expected, to have precisely the same effect as the timing change.

The effect of the boresight azimuth correction is illustrated in Figure 10. The first figure shows a histogram of the fine aspect observation residuals for a 5-day period with 5,710 star observations, using the prelaunch-measured boresight azimuth. The second plot shows the same data with the updated azimuth. The latest gyro calibrations were used for both cases. The plots illustrate the reduction in both the mean and the spread of the residuals. In the second case, the RMS residual is 1.2 arc-minutes, less than half of the fine aspect specification.

In retrospect, it might have seemed reasonable to include in the ground segment software a capability to determine the azimuth alignment directly, since it clearly impacts the fine aspect solution quality. However, the experience with the flight data shows that the observability of this parameter would have remained poor until the gyro propagation problems were resolved. At that point, determination of the correction became trivial; the most significant part of the effort was to verify the value over the duration of the mission.
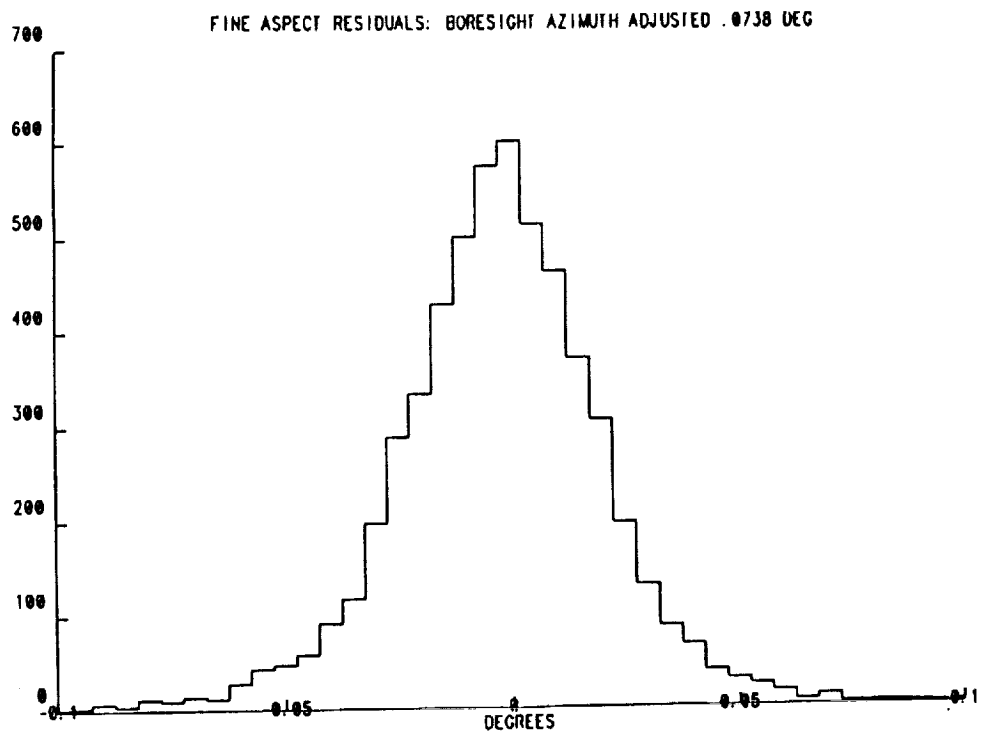
3.4 System Performance

The CDAC attitude processing software is designed to operate in an automated production processing environment. Typically, the system (a shared VAX 8820 computer) generates the attitude for a 24-hour data segment in about 1 hour. With the current system, the accuracy of the fine aspect is typically in the range of 1.5–2.0 arc-minutes for the 1989 and 1990 mission data.

At the beginning of 1991, the quality of the attitude solutions degraded because of the poor quality X-axis gyro data resulting from the degradation in the A_x gyro hardware performance. In March 1990 the X-axis gyros on the spacecraft were reconfigured to feed B_x gyro data into the telemetry for ground processing. At this time, the tuning of system parameters for data from B_x gyro is still in progress.

FINE ASPECT RESIDUALS DAYS 89356-361: DELAY= 3125
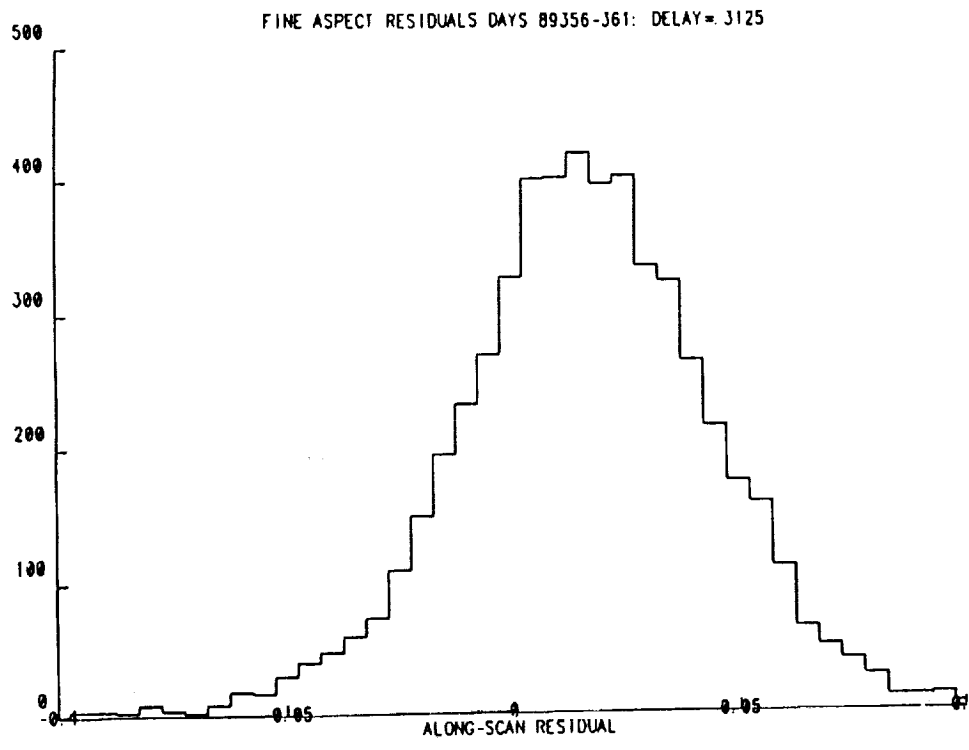
(a) Before DIRBE Boresight Alignment Adjustment

FINE ASPECT RESIDUALS: BORESIGHT AZIMUTH ADJUSTED .0738 DEG

(b) After DIRBE Boresight Alignment Adjustment

Figure 10. DIRBE Along Scan Residual Histogram

165

References

1.   "Spacecraft Attitude Determination and Control", Wertz, J.R., et al, D. Reidel Publishing Co., 1986

2.   "Low-precision Formulae for Planetary Positions", Van Flandern, T.C., and Pulkkinen, K. F., *The Astrophysical Journal*, November 1979

3.   "Cosmic Background Explorer (COBE) Attitude Ground Support Requirement Analysis", Computer Sciences Corporation report CSC/TM-84/6142, dtd. December 1984

4.   "Interface Control Document between FDF and the COBE Science Data Room (CSDR)", March 1990

5.   "COBE Ground Segment Gyro Calibration", Freedman, I., et al, *Proceedings of Flight Mechanics and Estimation Theory Symposium*, May 1991

6.   "COBE Attitude Determination System", Wright, E. L., et al, a poster paper presented at the AAS meeting in New Mexico, 1990

7.   "High Energy Astronomy Observatory-B (HEAO-B) Attitude Ground Support System (AGSS) Minor Frame Processor", Computer Sciences Corporation report CSC/TM-78/6006, dtd. January 1973

8.   "Two Micron Sky Survey", Neugebauer, G., and Leighton, R.B., NASA SP-3047, Washington, DC, 1969.

9.   "Three-Axis Attitude Determination from Vector Observations", *J. of Guidance, Control, and Dynamics*, Vol. 4, No. 1, January–February 1981, pp. 70–77.